Bioorganic & Medicinal Chemistry 21 (2013) 2687–2694

Contents lists available at SciVerse ScienceDirect

Bioorganic & Medicinal Chemistry

journal homepage: www.elsevier.com/locate/bmc

Neonicotinic analogues: Selective antagonists for α4β2 nicotinic acetylcholine receptors

Manuel Faundez-Parraguez [a], Nicolas Farias-Rabelo [a], Juan Pablo Gonzalez-Gutierrez [a], Alvaro Etcheverry-Berrios [a], Jans Alzate-Morales [b], Francisco Adasme-Carreño [b], Rodrigo Varas [c], Isabel Bermudez [d], Patricio Iturriaga-Vasquez [a,e,*]

[a] Department of Chemistry, Faculty of Sciences, University of Chile, Santiago, Chile
[b] Center for Bioinformatics and Molecular Simulation (CBSM), University of Talca, Talca, Chile
[c] Millennium Science Nucleus in Stress and Addiction and Faculty of Biological Sciences, Pontificia Universidad Católica de Chile, Santiago, Chile
[d] Department of Biological and Medical Sciences, Faculty of Health and Life Sciences, Oxford Brookes University, Oxford, UK
[e] Interdisciplinary Center for Ionic Liquids, University of Chile, Santiago, Chile

ARTICLE INFO

Article history:
Received 14 December 2012
Revised 8 March 2013
Accepted 16 March 2013
Available online 26 March 2013

Keywords:
Nicotinic acetylcholine receptors
Structure–activity relationships
Functional and affinities
Antagonism

ABSTRACT

Nicotine is an agonist of nicotinic acetylcholine receptors (nAChRs) that has been extensively used as a template for the synthesis of α4β2-preferring nAChRs. Here, we used the *N*-methyl-pyrrolidine moiety of nicotine to design and synthesise novel α4β2-preferring neonicotinic ligands. We increased the distance between the basic nitrogen and aromatic group of nicotine by introducing an ester functionality that also mimics acetylcholine (Fig. 2). Additionally, we introduced a benzyloxy group linked to the benzoyl moiety. Although the neonicotinic compounds fully inhibited binding of both [α-^{125}I]bungarotoxin to human α7 nAChRs and [^{3}H]cytisine to human α4β2 nAChRs, they were markedly more potent at displacing radioligand binding to human α4β2 nAChRs than to α7 nAChRs. Functional assays showed that the neonicotinic compounds behave as antagonists at α4β2 and α4β2α5 nAChRs. Substitutions on the aromatic ring of the compounds produced compounds that displayed marked selectivity for α4β2 or α4β2α5 nAChRs. Docking of the compounds on homology models of the agonist binding site at the α4/β2 subunit interfaces of α4β2 nAChRs suggested the compounds inhibit function of this nAChR type by binding the agonist binding site.

1. Introduction

Neuronal nicotinic acetylcholine receptors (nAChRs) are ligand-gated ion channels[1] expressed in the central and peripheral nervous systems[2] that respond to the neurotransmitter acetylcholine (ACh)[3] and exogenous compounds such as nicotine, cytisine and epibatidine[4,5] (Fig. 1). Neuronal nAChRs are predominantly located in extra-synaptic regions, from where they modulate the release of ACh and other neurotransmitters such as dopamine, GABA, glutamate, noradrenalin and serotonin,[6–8] which makes nAChR-signaling one of the most important modulatory system in the nervous system.[8,9] Mammalian neuronal nAChRs assemble from combinations of nine α (α2–α10) and three β (β2–β4) subunits.[4] Some of these subunits form homo-pentameric receptors such as α7 nAChRs, whilst other subunits assemble into hetero-pentameric structures with various combinations of α and β subunits.[10] Different subunit combinations yield functional nAChR that differ considerably in their functional and pharmacological properties.[11] The most abundant form of heteromeric nAChR in the brain contains α4 and β2 subunits (α4β2 nAChR). The α4 and β2 subunits also combine with other subunits such as α5 to form α4β2α5 nAChRs. α4β2 nAChRs bind nicotine with high affinity.[6] They have been implicated in nicotine self-administration, reward, nociception, mood and cognition, and in diseases such as Alzheimer's disease, epilepsy, pain disorders and depression.[6,10,12–14] Therefore, the perceived validity of α4β2 nAChR as therapeutic targets has stimulated the synthesis of a wide variety of novel compounds that have added to the list of nicotinic drugs and pharmacological tools.[10,15–17]

The crystal structure of a soluble ACh binding protein (AChBP) from *Aplysia californica* and other molluscs[18–20] has been used as a template to build homology models of the agonist binding domain of nAChRs.[21] The agonist binding domain in nAChRs is a hydrophobic pocket that lies at the interface between the extracellular N-terminal domains of two adjacent subunits.[4,10,21] In heteromeric nAChRs, α subunit contributes what is termed the principal

* Corresponding author. Tel.: +56 2 2978 7253; fax: +56 2 2271 3888.
E-mail address: iturriag@uchile.cl (P. Iturriaga-Vasquez).

0968-0896/$ - see front matter © 2013 Elsevier Ltd. All rights reserved.
http://dx.doi.org/10.1016/j.bmc.2013.03.024

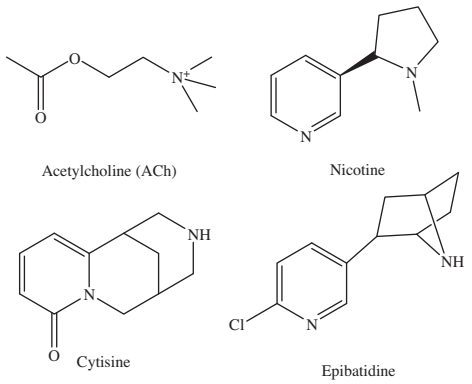

Figure 1. Classical nicotinic agonists.

component (or positive face), whereas the non-α subunit (β2 and β4 in neuronal nAChRs and γ, ε and δ in the muscle nAChR contribute the complementary component (or negative face). The principal component comprises loop A, B and C, whereas the complementary face consists of loops D, E and F.[22] In the case of homomeric nAChRs (e.g., α7 receptors), the α subunit contributes the primary and complementary faces of the agonist binding domain. Loop C, which is positioned at the entrance of the agonist binding domain, changes its conformation when an agonist or competitive antagonist binds, and this appears to be an essential part of the coupling mechanism that results in the opening of the ion channel.[23] Highly conserved aromatic residues that are critical for the binding of the neurotransmitter are located within loops A, B, C, D and E. These residues are Y93 (loop A), W149 (loop B), Y190 and Y198 (loop C), W55 and W57 (loop D). (Numbering of residues correspond to that of the *Torpedo* nAChR).[22] Generally, the identity of the hydrophobic residues on the principal component defines ligand affinity, whereas the residues contributed by the complementary face appear to determine ligand selectivity.[24] Typically, nicotinic agonists carry a positively charged nitrogen moiety that is stabilized by electronegative interactions with the conserved aromatic residues of the ligand binding site. Thus, the positive charged nitrogen moiety of ACh is stabilised by π–cation interactions with the electron rich aromatic side chain of the conserved amino acids, specifically W149.[25] Agonists also interact with other residues within the agonist site through a number of electronegative and hydrophobic interactions such as hydrogen bonding and van der Waals interactions.[20]

Guided by available information on how nicotinic ligands bind nAChRs and the chemical structure of nicotine, we synthesised simple molecules capable of interacting with the agonist binding site of α4β2 nAChRs via π–cation interactions. Here, we report the synthesis of a series of nicotine derivatives that preserve the *N*-methyl-pyrrolidine moiety of nicotine. We used as a lead molecule compound **1**, a previously described neonicotinic compound[10,26] (Fig. 2). The neonicotinic compounds shown in Figure 2 were synthesised by esterification reactions with substituted benzoic and nicotinic acid derivatives. We increased the distance between the basic nitrogen and the aromatic group of nicotine by introducing an ester functionality that also mimics acetylcholine (Fig. 2). Additionally, we introduced a benzyloxy group linked to the benzoyl moiety. Subsequent radioligand binding and functional assays in conjunction with homology modelling analysis showed that introduction of an ester group between the pyrrolidine moiety and the aromatic ring of nicotine confers antagonist properties to these ligands that selectively bind through π–cation interactions the agonist binding sites of α4β2 nAChRs. The compounds also interact with the agonist binding site of α7 nAChRs, albeit with lower affinity.

2. Results and discussion

2.1. Synthesis

The synthesis of the analogues was performed using the commercial (*S*)-(−)-1-methyl-2-pyrrolidinemethanol as a template for the pyrrolidine moiety of nicotine. Benzoyl chloride derivatives were prepared using thionylchloride as the halogenating reagent, with the exception of 6-chloronicotinoyl chloride, 4-bromo- and 4-chlorobenzoylchlorides that are commercially available from Aldrich. The corresponding acids were mixed with thionylchloride using dry THF as a solvent and refluxing for 24 h under N_2 atmosphere. Then, the solvent was evaporated under reduced pressure and the acyl chloride obtained was used immediately to minimize its hydrolysis. The resulting acylchloride was dissolved in dry diethyl ether with stirring and (*S*)-(−)-1-methyl-2-pyrrolidinemethanol was added drop by drop to obtain the corresponding esters. To obtain benzyloxy derivatives attached to the corresponding 4-hydroxybenzoate or 6-hydroxynicotinates, we used a Fischer esterification reaction to yield the corresponding methyl ester,[27] followed by the Williamson ether synthesis using benzylchloride and $NaHCO_3$ in acetonitrile.[28] Then a basic Fischer hydrolysis produced the O-benzylated aromatic acid. This strategy was used to minimize the problem posed by the insolubility of acids in the Williamson synthesis, since in the presence of a base such as $NaHCO_3$ a precipitate forms, reducing the reaction yield considerably (Fig. 3).

To obtain the 3-aminobenzoyl derivative we used the classical aromatic electrophilic nitration of methyl benzoate by a concentrated sulphuric–nitric acid mixture. This reaction produced the nitro derivative in high yields, and the reaction product crystallized in the reaction mixture. To obtain the 3-nitrobenzoyl ester of (*S*)-(−)-1-methyl-2-pyrrolidinemethanol, the reaction was conducted as mentioned above. The nitro group was reduced via catalytic hydrogenation using 10% Pd/C in ethanol, which proved to be a faster and cleaner way of generating the aromatic amino group (Fig. 4).

2.2. Biological evaluation

2.2.1. Radioligand binding studies

First, we determined binding affinities (K_i) of the synthesised neonicotinic compounds for human α4β2 nAChRs and human α7 nAChRs using respectively [^{3}H]cytisine ([^{3}H]cyt) and [^{125}I]α-bungarotoxin (α-BgTx) binding competition assays to evaluate the nAChR selectivity of the compounds. These radioligands are established nicotinic ligands that bind the agonist site of, respectively α4β2 nACRs and α7 nAChRs.[29,30] The assays were carried out on membrane homogenates prepared from SH-EP1-hα4β2 clonal cells or SH-SY5Y-hα7 clonal cells. It has been shown previously that SH-SY5Y-hα7 cells over-express human α7 nAChRs and that SH-EP-hα4β2 cells express human α4β2 nAChRs.[31–33] The latter cell line is likely to express alternate forms of the α4β2 nAChR, namely $(\alpha4\beta2)_2\alpha4$ and $(\alpha4\beta2)_2\beta2$.[34] The K_d for [^{125}I]α-BgTx (1 ± 0.2 nM) binding to α7 nAChRs and [^{3}H]cyt binding to α4β2 nAChRs (0.43 ± 0.08 nM) were comparable to previously published data.[33] Figure 5 shows that specific binding of both [^{125}I]α-BgTx to α7 nAChRs and [^{3}H]cyt to α4β2 nAChRs was fully displaced by the synthesised compounds in a concentration-dependent and monophasic manner. This pattern of inhibition strongly suggests that the compounds bind the agonist site of the receptors. The K_i values estimated for the affinity of the compounds for α4β2 and α7 nAChRs are shown in Table 1. For comparison we include the affinity of nicotine for both receptor types. All the compounds tested were significantly more potent at α4β2 nAChRs than at α7 nAChRs. Despite the differences in affinity, the pattern of affinity change obtained by incorporating various types of substituents into

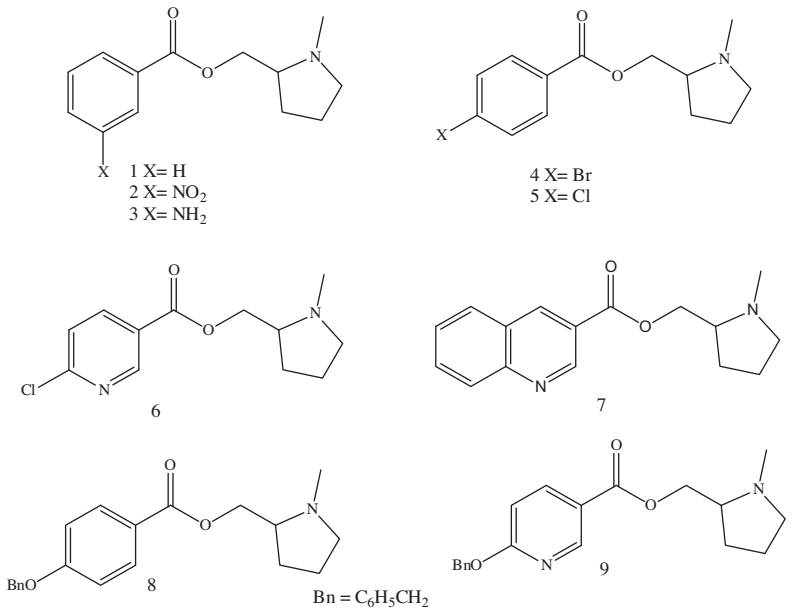

Figure 2. Simple neo-nicotinic analogues synthesised in this study.

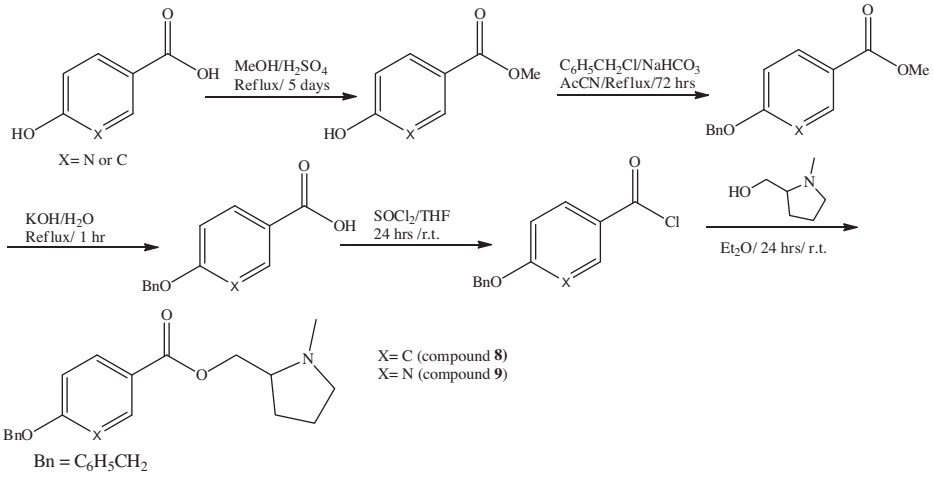

Figure 3. Synthesis of benzyloxy derivatives compounds **8** and **9**.

compound **1** was comparable in both receptor types, except for compound **3**. Thus, compound **8** showed the highest affinity in the series with a K_i of 1.2 nM α4β2 nAChRs and of 1.1 μM at α7 nAChRs. In contrast, the pyridyl analogue **9** was markedly less potent at both receptor types, suggesting that in this molecule the presence of a pyridyl group leads to an unfavourable interaction with the agonist binding site in both α4β2 and α7 nAChRs. The presence of a nitro group (**2**) or a quinoline (**7**) moiety decreases affinity in comparison to compound **1** at both receptor types. Additionally, we tested two 4-halobenzoate derivatives (compounds **4** and **5**) and the 6-chlorinicotinate analogue **6**. The binding affinities at α4β2 nAChRs show that both 4-halobenzoate derivatives **4** and **5** bind at nanomolar concentrations (K_i 22.4 and 11.2 nM, respectively), but the chloronicotinate derivative **6** had an almost tenfold lower affinity compared with **5** (151 nM vs 11.2 nM) (Table 1). Of all the compounds tested, **5** displayed high affinity at α7 nAChRs (K_i 4.5 μM) followed by **1** and **4** (K_i 6.7 μM and K_i 10.5 μM respectively) (Table 1). Taken together, the binding data demonstrate that the synthesised compounds display higher selectivity for α4β2 nAChRs than for α7 nAChRs.

2.2.2. Functional studies

Next, we determined the functional effects of the most potent neonicotinic compounds (compounds **1**, **3**, **5** and **8**) on α4β2n AChRs expressed heterologously in *Xenopus* oocytes. The studies were carried out using two-electrode voltage clamping procedures described in the Section 4. We assayed the effects of the compounds on three different subtypes of α4β2 nAChRs, namely $(\alpha4\beta2)_2\beta2$, $(\alpha4\beta2)_2\alpha4$ and $(\alpha4\beta2)_2\alpha5$ nAChRs. These α4β2 nAChRs display different functional sensitivity to nicotinic ligands,[34–36] and they all likely express in the brain.[37] All of the compounds tested inhibited the currents evoked by ACh at $(\alpha4\beta2)_2\beta2$, $(\alpha4\beta2)_2\alpha4$ or $(\alpha4\beta2)_2\alpha5$ nAChRs. Estimated IC_{50} values are summarised in Table 2. For comparison, we include IC_{50} values estimated for the α4β2-preferring competitive antagonist dihydro-β-erythroidine (DhβE) (Table 2). Compounds **1**, **3** and **5** displayed marked α4β2 nAChR subtype selectivity. Thus, compounds **1** and **5** had higher inhibitory potency at $(\alpha4\beta2)_2\beta2$and $(\alpha4\beta2)_2\alpha5$ than at $(\alpha4\beta2)_2\alpha4$, whereas compound **3** showed marked preference for $(\alpha4\beta2)_2\alpha4$ and $(\alpha4\beta2)_2\beta2$ nAChRs. The latter compound is particularly interesting because it discriminates between $(\alpha4\beta2)_2\beta2$ and $(\alpha4\beta2)_2\alpha5$ nAChRs. In general,

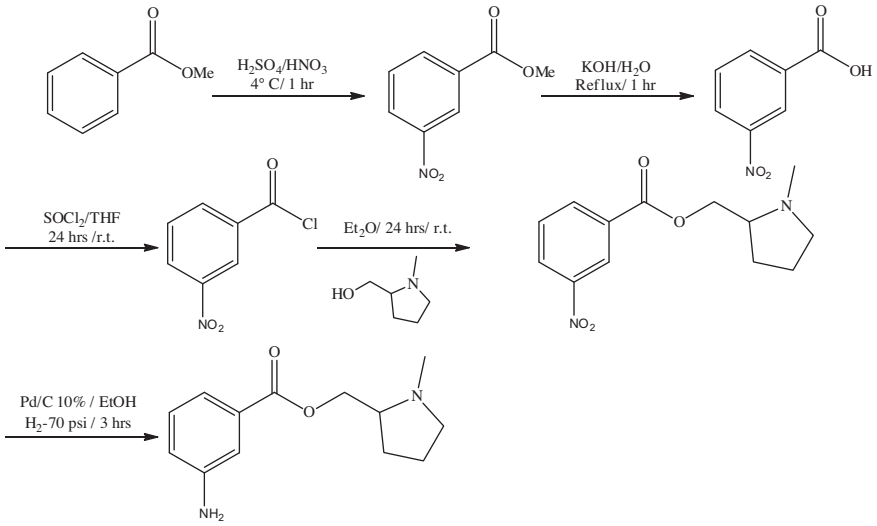

Figure 4. Synthesis of 3-nitro and 3-amino derivatives compounds **2** and **3**.

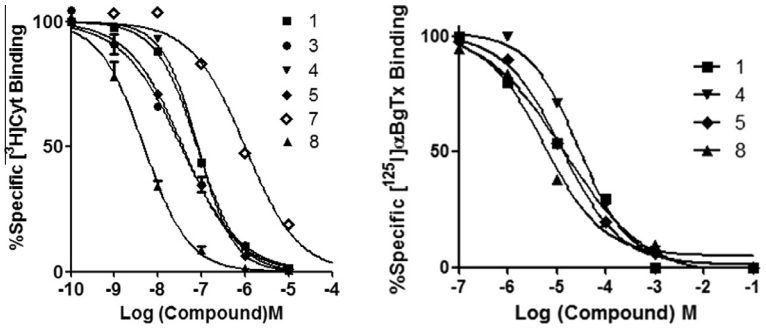

Figure 5. Effects of neonicotinic compounds on binding of [^{3}H]cytisine to human α4β2 nAChRs and [^{125}I]-α-bungarotoxin to human α7 nAChRs. Data points represent the mean ± SEM of four experiments, each carried out in triplicate. The radioligand concentration in all displacement studies was 1 nM. The concentration-inhibition data was analysed non-linearly as described in Section 4.

Table 1
Comparisons of binding affinities of neonicotinoid compounds at human α7 and α4β2 nAChRs

Compound	α4β2 IC_{50} (nM)	α4β2 K_i (nM)	α7 IC_{50} (μM)	α7 K_i (μM)
Nicotine	1.2	0.6	7.6	3.8
1	81.9 ± 5	23.4 ± 6	13.4 ± 1	6.7 ± 1
2	1611 ± 12	460 ± 8	464 ± 17	232 ± 7
3	28.4 ± 3	8.1 ± 1	N.E.	
4	78.4 ± 6	22.4 ± 3	21.1 ± 4	10.5 ± 2
5	39.4 ± 5	11.2 ± 2	8.9 ± 5	4.5 ± 0.8
6	528 ± 10	151 ± 5	58.5 ± 7	29.3 ± 2
7	759 ± 9	217 ± 6	97.3 ± 6	48.7 ± 3
8	4.2 ± 0.8	1.2 ± 0.3	2.3 ± 0.6	1.1 ± 0.4
9	166 ± 7	45.5 ± 4	59.1 ± 3	29.5 ± 3

Data represent the mean ± SEM of four experiments, each with triplicate samples. For comparison we include equivalent K_i and IC_{50} estimates for nicotine. The radioligand concentration in all displacement studies was 1 nM and the equilibrium dissociation constants (K_d) used to estimate K_i values were 1 nM for [^{125}I]α-BgTx binding to human α7 nAChRs and 0.4 nM for the binding of [^{3}H]cyt to human α4β2 nAChRs. K_d values were determined as indicated in the Section 4. N.E. no effects at the highest concentration tested (1 mM).

Table 2
Inhibitory potency of neonicotinoid compounds at α4β2 nAChRs

Compound	$(\alpha4\beta2)_2\beta2$ (μM)	$(\alpha4\beta2)_2\alpha4$ (μM)	$(\alpha4\beta2)_2\alpha5$ (μM)
1	2.5 ± 0.9	313 ± 12	52.3 ± 4
3	4.3 ± 0.6	1.02 ± 0.4	480 ± 8
5	3.6 ± 0.7	95 ± 2	6.0 ± 1
8	25.8 ± 1.2	3.6 ± 0.7	17.8 ± 0.9
DhβE	0.41	0.02	0.011

The effects of the compounds were studied on $(\alpha4\beta2)_2\beta2$, $(\alpha4\beta2)_2\alpha4$ and $(\alpha4\beta2)_2\alpha5$ nAChRs expressed heterologously in *Xenopus* oocytes as described elsewhere. The inhibitory potency of the α4β2-preferring competitive antagonist dihydro-β-erythroidine (DhβE) is included for comparison.

$(\alpha4\beta2)_2\beta2$ and $(\alpha4\beta2)_2\alpha5$ nAChRs display comparable sensitivity for competitive nicotinic ligands[36] (Table 2). Thus, introducing an amino group at the *meta* position of the aromatic ring in compound **1** (compound **3**) decreases potency at $(\alpha4\beta2)_2\alpha5$ nAChRs by about 10-fold without significantly affecting the inhibitory potency at $(\alpha4\beta2)_2\beta2$ nAChRs. The presence of the amino group also increased the inhibitory potency of compound **1** at $(\alpha4\beta2)_2\alpha4$ nAChRs, bringing it closer to that displayed at $(\alpha4\beta2)_2\beta2$ nAChRs. Chlorination of the aromatic ring of compound **1** at the 4 position (compound **5**) increased slightly the inhibitory potency at $(\alpha4\beta2)_2\alpha4$ nAChRs (from 313 to 95 μM), whereas at $(\alpha4\beta2)_2\alpha5$ nAChRs it increased it by almost 10-fold without affecting potency at $(\alpha4\beta2)_2\beta2$ nAChRs. Of all compounds tested, compound **8**, the bulkiest molecule of the group tested, displayed the least α4β2 nAChR subtype selectivity. Thus, even though compound **8** was more potent at inhibiting $(\alpha4\beta2)_2\alpha4$ nAChRs (IC_{50} of 3.6 μM), its inhibitory potency at $(\alpha4\beta2)_2\beta2$ and $(\alpha4\beta2)_2\alpha5$ nAChRs decreased by only 5 and 7 times, respectively (Table 2). Taken together, the findings suggest that a positive nitrogen atom at the meta position in compound **1** (compound **3**) increases selectivity for $(\alpha4\beta2)_2\beta2$ and $(\alpha4\beta2)_2\alpha4$

but decreases it for $(\alpha4\beta2)_2\alpha5$ nAChRs. In contrast, substitutions in position 4 of the aromatic ring of compound **1** tend to decrease α4β2 receptor selectivity by increasing the inhibitory potency at $(\alpha4\beta2)_2\alpha4$ and $(\alpha4\beta2)_2\alpha5$ nAChRs closer to that displayed at $(\alpha4\beta2)_2\beta2$ nAChRs. These results highlight interesting differences in the receptor subtype selectivity of the compounds tested, which suggest that the ligand binding domain of $(\alpha4\beta2)_2\beta2$ nAChRs is less discriminatory than its counterparts on $(\alpha4\beta2)_2\alpha4$ or $(\alpha4\beta2)_2\alpha5$ nAChRs.

2.3. Docking studies

The radioligand displacement studies suggested that the compounds have higher affinity for the binding site of α4β2 nAChRs than for that of α7 nAChRs. In an attempt to explain the differences in binding affinity and functional potency of the neonicotinoid compounds at α4β2 nAChRs, we performed docking calculations with the compounds on homology models of the α4β2 nAChR agonist binding site. The extracellular N-terminal ligand binding domain of the α4β2 nAChR was modeled using the X-ray structure of the AChBP from *Aplysia californica* (Protein Data Bank codes 2BYN and 1UW6)[19,21] as a template. α4β2 nAChR homology models were obtained in both the open and closed-channel states. All the neonicotinoid compounds were docked into the α4(+)/β2(−) interface centering the grid on α4W182. This residue is equivalent to α1W149 on the muscle nAChR, whichs π–cation interacts with the quaternary ammonium group of ACh[25] affecting agonist binding affinity.[38] The position of loop C in the open and close conformations used to evaluate the binding energies of the ligand dockings. The docking results indicate that small changes in the nicotine structure such as addition of an ester link and other modifications in the aromatic ring lead to unfavourable interactions with the agonist binding site. Thus, the docking energies predicted do not favour interactions between such ligands and the agonist binding site. However, when we performed the same docking analysis with loop C in the open conformation, all the neonicotinoid compounds appear to dock into the agonist site with considerably high energies (−8 to −12 kcal/mol) indicating higher affinities for this conformational state of the α4β2 nAChR. The binding modes of the nicotine derivatives suggest that the principal interactions stabilising binding of the compounds to the agonist binding site are between the protonated nitrogen of the pyrrolidine moiety and the W182 residue (Fig. 6). Our docking results are thus consistent with the findings of the radioligand and functional assays that suggest the synthesised nicotine derivatives inhibit the function of α4β2 nAChRs by binding to the agonist binding site.

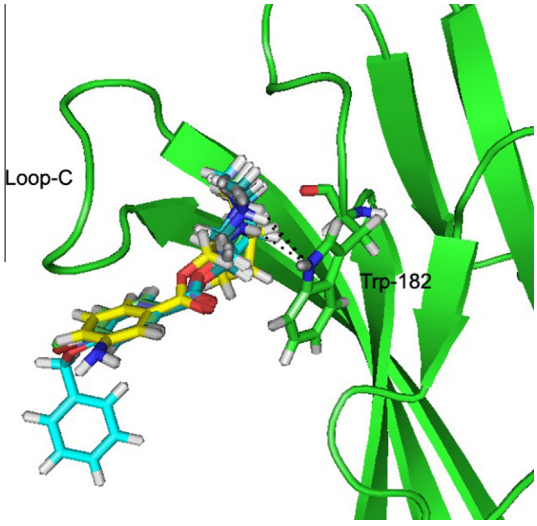

Figure 6. Superimposition of compounds **1**, **3**, **4** and **8** in the binding site of the α4β2 nAChR. The image shows the π–cation interaction between the ligands and α4W182 in the closed channel state conformation (loop C open).

3. Conclusions

Herein we have combined radioligand binding assays, functional characterisation and homology modelling to define the mode of action and selectivity of novel neonicotinic compounds at α7 and α4β2 nAChRs. The radioligand binding assays demonstrated that the synthesised compounds are α4β2-preferring ligands. The compounds fully displaced the binding of [^{125}I]α-BgTx to α7 nAChRs and [^{3}H]cyt to α4β2 nAChRs, suggesting that the compounds interact directly with the agonist binding site of these nAChRs. This possibility is consistent with our docking data that shows that the pyrrolidine moiety present in our molecules interacts with the agonist binding site of α4β2 nAChRs via π–cation coupling. The subtype selectivity of our molecules appears to be defined by the pyrrolidine moiety as it appears to be the case for nicotine, which displays higher affinity for α4β2 nAChRs than for α7 nAChRs.[16]

Despite the submicromolar affinities shown by this pyrrolidine series, we found that just five of the compounds (**1**, **3**, **4**, **5** and **8**) tested have K_i values under 100 nM. With the exception of compound **8** that contains a benzyloxy group at the *para* position of the benzoate moiety, bulky compounds such as **7**, **9**, showed poor affinities. The presence of the pyridine group in some molecules decreased affinity markedly, indicating an unfavourable interaction with the protein for this kind of molecules, in contrast to nicotine. The high affinity of compound **8**, results from a favourable interaction of the benzyloxy group in the aromatic cage of the binding site plus the π–cation interaction of the pyrrolidine-W182 couple. The chlorine atom in compound **5** is better for affinity than a bromine atom at the same position. The amino group at the *meta* position in compound **3**, increases affinity compared to **1**, but in contrast a nitro group, compound **2** decreases its affinity drastically.

All the compounds tested behaved as antagonists of α4β2 nAChRs. Although by comparison to the α4β2-preferring competitive antagonist DhβE the synthesised neonicotinoids are moderate inhibitors of α4β2 nAChRs, they display interesting α4β2 nAChR stoichiometry-selectivity. Thus, for example, compounds **1** and **5** display preference for $(\alpha4\beta2)_2\beta2$ and $(\alpha4\beta2)_2\alpha5$ nAChRs, whereas compound **3** shows marked preference for $(\alpha4\beta2)_2\beta2$ and $(\alpha4\beta2)_2\alpha4$ nAChRs. This selectivity is intriguing because the agonist site at the two α4/β2 subunit interfaces of these three receptor types are structurally identical.[39] Recently, however, it has been shown that $(\alpha4\beta2)_2\alpha4$ are endowed with a third operational agonist site at the α4/α4 interface that is responsible for the signature sensitivity for competitive and allosteric ligands of the $(\alpha4\beta2)_2\alpha4$ receptor isoform.[39] Binding or lack of binding to this additional site may explain the selectivity of the compounds for the $(\alpha4\beta2)_2\alpha4$ isoform. Little is known of the role of receptor specific subunit interfaces in $(\alpha4\beta2)_2\beta2$ or $(\alpha4\beta2)_2\alpha5$ but considering that the aromatic residues that contribute to α/β agonist sites are highly conserved in nAChRs subunits, it may be that the receptor selectivity of the neonicotinic antagonists results from interactions with additional sites in the receptors. Further substitutions on the aromatic ring of compound **1** are thus likely to lead to a better understanding of the receptor selectivity and the structural relationships for derivatives of compound **1** at the α4β2 nAChR family. In summary, our results indicate that for this series of compounds there are some structural requirements that confer selectivity for heteromeric nAChR subtypes rather than for the homomeric subtype. Additionally, we found interesting information about the subtype selectivity for $(\alpha4\beta2)_2\beta2$, $(\alpha4\beta2)_2\alpha4$ and $(\alpha4\beta2)_2\alpha5$ nAChRs.

4. Materials and methods

4.1. Clonal cell lines

The SH-SY5Y-hα7 cell line, over-expressing human α7 nicotinic acetylcholine receptors, was created as previously described[31–33] and used to assay [^{125}I]-α-BgTx binding. Membrane homogenates for [^{3}H]cyt binding studies were prepared from the SH-EP-hα4β2 clonal cell line, which express human α4β2 NAChRs.[32,33] Cells were maintained in Dulbecco's modified Eagle's medium (Invitrogen, UK) supplemented with 5% foetalcalfserum, 10% horseserum, 2 mM L-glutamine, 10 IU/mL penicillin, 10 μg/mL streptomycin, 2.5 μg/mL amphotericin B and 0.4 mg/mL hygromycin. For SH-EP-hα4β2 culture media, the hygromycin concentration was decreased to 130 μg/mL, and zeocin (Invitrogen, UK) was added at 250 μg/mL.

4.2. Ligand binding assays

Competition binding studies were performed on membrane homogenates prepared from SH-SY5Y-hα7 clonal cell line or SH-EP1-hα4β2 clonal cell line, using [I^{125}]α-BgTx (PerkinElmer, UK) or [^{3}H]cyt (PerkinElmer, UK) respectively, as previously described.[33] Membrane homogenates were incubated at a final protein concentration of 30–50 μg per assay tube in a final volume of 500 μL ([125I]α-BgTx) or 250 μL ([3H]cyt) of binding saline (in nM: 120 NaCl, 5 KCl, 1 $MgCl_2$, 2.5 $CaCl_2$, 50 Tris, pH 7.0) for 120 min at room temperature (25 °C) with 1 nM [I^{125}]α-BgTx or for 75 min at 4 °C with 1 nM [^{3}H]cyt. For both binding assays, 10 μM nicotine was used to define nonspecific binding. Bound and free fractions were separated by rapid filtration through Whatman GF/C filters pre-soaked in binding saline supplemented with 0.1% polyethyleneimine. Radioactivity was quantified by liquid scintillation spectrometry.

4.3. Electrophysiological recordings

Concatenated $(\alpha4)_2(2)_3$, $(\alpha4)_3(\beta2)_2$ and α4β2α5 receptors were expressed heterologously in *Xenopus* oocytes as previously described.[34,35] The order of subunits in the concatenated receptors was β2_α4_β2_α4_β2 for $(\alpha4)_3(2)_2$, β2_α4_β2_α4_α4 for $(\alpha4)_3(\beta2)_2$ and α5_β2_α4_β2_α4 for α4β2α5 receptors. Oocytes were placed in a 0.1 mL recording chamber and perfused with Ringer solution (in mM: NaCl 150, KCl 2.8, Hepes 10, $CaCl_2$ 1.8; pH 7.2, adjusted with NaOH) at a rate of 15 mL/min. Oocytes were impaled by two microelectrodes filled with 3 M KCl (0.3–2.0 MΩ) and voltage-clamped at −60 mV using a Geneclamp 500B amplifier. Typically current traces were filtered at 1 kHz during recording and digitized at 1 kHz using the DigiData 1200 interface for subsequent analysis using PClamp 8 software (Axon Instruments, CA, USA). All experiments were carried out at room temperature. Compounds were applied by gravity perfusion using a manually activated valve. ACh concentration-response curves were obtained by normalizing ACh-induced currents to the control responses induced by 1 mM ACh (a near-maximum effective concentration at $(\alpha4\beta2)_2\alpha4$ nAChRs but a maximal concentration at $(\alpha\beta2)_2\beta2$ or $(\alpha4\beta2)_2\alpha5$ nAChRs.[34–36] A minimum interval of 4 min was allowed between ACh applications as this was found to be sufficient to ensure reproducible recordings. The sensitivity of the receptors to inhibition by antagonists was tested by first superfusing the antagonist for 2 min and then co-applying it with an EC_{50} concentration of ACh (100 μM for $(\alpha4\beta2)_2\alpha4$ nAChRs and 2 μM for $(\alpha\beta2)_2\beta2$ or $(\alpha4\beta2)_2\alpha5$ nAChRs). Antagonist concentration response data were normalized to the appropriate ACh EC_{50} constant responses to ACh were obtained before the co-application of ACh and compound. To maintain on-going measurements of the control response to ACh throughout the experiment, each co-application was bracketed by an application of EC_{50} of ACh alone.

4.4. Homology modeling

The agonist binding domain of the α4β2 nAChR was modeled using as a template the crystal structures of the AChBP from *Aplysia californica* in the close and open states (Protein Data Bank codes: 2BYN and 1UW6, respectively).[19,21] Even though the sequence identity between AChBP and the subunits of the α4β2 nAChRs is only 18–20%, a similar fold and highly-conserved binding site residues make the AChBP structure suitable for modeling the agonist binding site of nAChRs. The sequences of human nAChR α4 (P43681) and β2 (P17787) subunits were obtained from the ExPASy Server. Multiple sequence alignment was performed using ClustalW[40] and 200 models of each α4 and β2 nAChRs subunits were generated using Modeller 8.[41]The overall average g factor for the best structures was −0.20. This value is a good indicator for the quality of the models. Each sub-unit was separately constructed and then relaxed by 1 nanosecond (ns) long molecular dynamics simulation with Desmond[42,43] molecular dynamic software in a solvated SPC[44] and neutralized system. Receptor assembly was made by superposition, of relaxed-subunit replicas, against the available AChBP crystal structure templates and following the $(\alpha4\beta2)_2\beta2$ stoichiometry. All the generated homology models possess an explicit disulfide bond between α4 residues C225 and C226 and reproduce the amino acids previously reported as implicated in agonist binding by nAChR.[4,21] The whole α4β2 nAChR model was energy-minimized and equilibrated in explicit solvent, using long molecular dynamic (MD) simulations. All simulations were performed using the Desmond molecular simulation package[42,43] and OPLS 2005[44] all-atom force field with explicit solvent and employing the single point charge (SPC) water model. Detailed information about the system setup and MD protocol followed in this study can be found in Muñoz et al.[45] Images were generated using PyMOL software. The best model was energy-minimized in vacuo, using Desmond molecular dynamic software and the OPLS 2005 force field with explicit solvent.

4.5. Docking analysis

Molecular docking of the nicotine analogues at the agonist binding domain of the α4β2 homology models was investigated using the Lamarckian genetic algorithm search method using software AutoDock v4.0.[46] The receptors were kept rigid, while full flexibility was allowed for the ligands to translate/rotate. Polar hydrogens were added to the receptors and Kollman-united atom partial charges along with atomic solvation parameters were assigned to the individual protein atoms. The three-dimensional structures of each ligand were generated using the SPARTAN'08 program and were then energy minimized. For each ligand, a rigid root and rotatable bonds were assigned automatically. The non-polar hydrogens were removed and the partial charges from these were added to the carbons (Gasteiger charges). The atom type for aromatic carbons was reassigned in order to use the AutoDock 4.0 aromatic carbon grid map. Docking was carried out using $60 \times 60 \times 60$ grid points with a default spacing of 0.375 Å. The grid was positioned to include the full ligand binding pocket in the central part of the α4β2 subunit interfaces so as to allow extensive sampling around residue α4W182 (W143 in mature AChBP). Within this grid, the Lamarckian genetic search algorithm was used with a population size of 150 individuals, calculated using 200 different runs (i.e. 200 dockings). Each run had two stop criteria, a maximum of 1.5×10^6 energy evaluations or a maximum of 50,000 generations, starting from a random position and conformation; default parameters were used for the Lamarckian genetic algorithm search.

4.6. Data analysis

Concentration-response data for antagonists were fitted by nonlinear regression (Prism 5.0, GraphPad, USA) to the equation $i = i_{max}/[1+(IC_{50}/x)^{nHill}]$ wherein i_{max} = maximal normalized current response (in the absence of antagonist for inhibitory currents), x = antagonist concentration, IC_{50} = antagonist concentration eliciting half-maximal inhibition and nHill = Hill coefficient. Results are presented as mean ± standard error of the mean (SEM) of at least four separate experiments from at least two different batches of oocytes. The same equation was used to estimate IC_{50} values for inhibition of radioligand binding and the K_i value of the test compounds was determined using the equation of Cheng and Prusoff: $K_i = IC_{50}/1+[x]/K_D$, wherein x is the radioligand concentration and K_D the affinity binding constant. Statistical significance was assessed using a two-tailed unpaired *t*-test, or one-way analysis of variance (ANOVA). *P* values less than 0.05 were considered significant.

5. Chemistry

Melting points are uncorrected and were determined with a Reichert Galen III hot plate microscope. ^{1}H NMR spectra were recorded using Bruker AMX 400 spectrometers at 400 MHz. Chemical shifts are reported relative to TMS (δ = 0.00) or HDO (δ = 4.79) and coupling constants (*J*) are given in Hz. IR spectra were recorded on a Bruker Vector 22 spectrophotometer using KBr. The elemental analyses for C, H, N were performed on a CE Instruments (model EA 1108) analyzer. Reactions and product mixtures were routinely monitored by thin-layer chromatography (TLC) on silica gel-precoated F_{254} Merck plates, normally we use a mixture of $CHCl_3$/CH_3OH as a mobile phase. All reagents and solvents were commercially available and were used without further purification.

5.1. General procedures

5.1.1. Synthesis of benzyloxy derivatives

6-Hydroxybenzoic acid and 6-hydroxynicotinic acid were previously transformed in their corresponding methyl esters, using methanol–sulfuric acid under reflux by 5 days. Methyl esters were benzylated using benzyl chloride in acetonitrile as solvent and $NaHCO_3$, the mixture was kept under reflux for 3 days. After this time, the solvent was evaporated and the benzyloxy esters were hydrolyzed in KOH by refluxing for 1 h. benzyloxy acids were purified by column chromatography using Silica gel 60 and a mobile phase of $CHCl_3$/CH_3OH (90/10).

5.1.2. Synthesis of benzoyl chlorides

The corresponding benzoic acids were converted into benzoyl chlorides using thionylchloride as a halogenating agent, and the reaction was performed with each of the corresponding benzoic acids (6–10 mmol) and 5 mL of thionyl chloride using dry THF as a solvent, under a nitrogen atmosphere. The mixture was maintained at room temperature for 24 h, and then the solvent, excess reagents and remaining HCl and SO_2 were evaporated under vacuum. The unpurified benzoyl chloride was used immediately for the next reaction.

5.1.3. Synthesis of ((*S*)-1-methylpyrrolidin-2-yl)methyl benzoates

Benzoyl chlorides were dissolved in 50 mL of diethyl ether and stirred at room temperature. One equivalent of (*S*)-1-methylpyrrolidin-2-ylmethanol (around 0.3-0.4 mL) in 30 mL of diethyl ether was added drop by drop. The reaction mixture was kept at room temperature with constant stirring for 24 h. Then, the solvent was evaporated, the mixture was re-dissolved in water, adjusted to pH 8.0 and extracted with CH_2Cl_2. The hydrochloride salt was obtained from acetone.

5.1.4. ((*S*)-1-Methylpyrrolidin-2-yl)methyl benzoate (1)

Prepared in the similar way as described above in general procedures. (*S*)-(−)-1-Methyl-2-pyrrolidinylmethanol (4.0 mmol, 0.5 mL) was added to a solution of benzoyl chloride (4.0 mmol, 0.49 mL). Yield 816 mg (76%), mp 165.4–169.0 °C, ^{1}H NMR (400 MHz, D_2O) δ 7.28 (m, 2H), 6.93 (m, 2H), 4.13 (dd, *J* = 9.6, *J* = 5.6 Hz, 1H), 3.95 (dd, *J* = 9.6, *J* = 5.4 Hz, 1H), 3.24 (m, 1H), 2.83 (m, 1H), 2.58 (s, 3H), 2.44 (m, 1H), 2.09 (m, 1H), 1.93 (m, 1H), 1.82 (m, 2H). ^{13}C NMR (100 MHz, D_2O) δ 167.1, 133.1, 130.2, 129.9 (2C), 128.7 (2C), 65.4, 64.9, 57.9, 40.6, 28.1, 23.1. IR (KBr, cm^{-1}) 2978, 1720, 1279, 1112. Anal. Calcd for $C_{13}H_{18}ClNO_2$: C, 61.05; H, 7.09; N, 5.48. Found: C, 61.35; H, 7.19; N, 5.53.

5.1.5. ((*S*)-1-Methylpyrrolidin-2-yl)methyl 3-nitrobenzoate (2)

Prepared in the similar way as described in general procedures. (*S*)-(−)-1-Metil-2-pirrolidinilmetanol (4.0 mmol, 0.5 mL) was added to a solution of 3-nitrobenzoyl chloride (4.0 mmol, 783 mg). Yield 822 mg (65%), mp 171–174 °C, ^{1}H NMR (400 MHz, D_2O) δ 7.81 (d, *J* = 8.1 Hz, 1H), 7.75 (s, 1H), 7.42 (t, *J* = 8.2 Hz, 1H), 7.25 (d, *J* = 8.1 Hz, 1H), 4.05 (dd, *J* = 9.0, *J* = 5.4 Hz, 1H), 3.98 (dd, *J* = 9.2, *J* = 5.3 Hz, 1H), 3.19 (m, 1H), 2.52 (s, 3H), 2.32 (m, 1H), 2.06 (m, 1H), 2.09 (m, 1H), 1.82 (m, 3H). ^{13}C NMR (100 MHz, D_2O) δ 168.9, 148.3, 136.2, 131.1, 129.6, 125.6, 124.8, 65.4, 64.9, 57.9, 40.6, 28.1, 23.1. IR (KBr, cm^{-1}) 2980, 1715, 1550, 1350, 1266, 1108. Anal. Calcd for $C_{13}H_{17}ClN_2O_4$: C, 51.92; H, 5.70; N, 9.31. Found: C, 51.83; H, 5.61; N, 9.27.

5.1.6. ((*S*)-1-Methylpyrrolidin-2-yl)methyl 3-aminobenzoate (3)

3-Aminobenzoate derivative was prepared by catalytic hydrogenation of the corresponding ((*S*)-1-methylpyrrolidin-2-yl)-methyl 3-nitrobenzoate (compound **2**) (8.0 mmol, 2.0 g) using Pd-C 10% in ethanol at 70 psi by 3 h. Yield 1.71 g (95%), mp 172–176 °C, ^{1}H NMR (400 MHz, D_2O) δ 7.31 (d, *J* = 8.3 Hz, 1H), 6.90 (d, *J* = 8.3 Hz, 1H), 6.83 (d, *J* = 8.3 Hz, 1H), 6.81 (s, 1H), 4.33 (dd, *J* = 11.3, *J* = 3.0 Hz, 1H), 4.15 (dd, *J* = 11.2, *J* = 5.9 Hz, 1H), 3.76 (m, 1H), 3.59 (m, 1H), 3.12 (m, 1H), 2.88 (s, 3H), 2.26 (m, 1H), 2.09 (m, 1H), 1.95 (m, 3H).^{13}C NMR (100 MHz, D_2O) δ 163.9, 148.2, 131.2, 129.1, 120.6, 119.6, 114.3, 65.4, 64.9, 57.9, 40.6, 28.1, 23.1. IR (KBr, cm^{-1}) 3442, 3360, 2978, 1730, 1626,1285, 1270, 1115. Anal. Calcd for $C_{13}H_{19}ClN_2O_2$: C, 57.67; H, 7.07; N, 10.35. Found: C, 57.74; H, 7.12; N, 10.46.

5.1.7. ((*S*)-1-Methylpyrrolidin-2-yl)methyl 4-bromobenzoate (4)

Prepared in the similar way as described above in general procedures. (*S*)-(−)-1-Methyl-2-pyrrolidinylmethanol (4.0 mmol, 0.5 mL) was added to a solution of 4-bromobenzoyl chloride (4.0 mmol, 926 mg). Yield 981 mg (78%), mp 231.4–232, 1 °C, ^{1}H NMR (400 MHz, D_2O) δ 7.91 (d, *J* = 8.8 Hz, 2H), 7.49 (d, *J* = 8.8 Hz, 2H), 4.67 (dd, *J* = 13.6, *J* = 2.9 Hz, 1H), 4.52 (dd, *J* = 13.5, *J* = 6.6 Hz, 1H), 3.90 (m, 1H), 3.75 (m, 1H), 3.26 (m, 1H), 2.98 (s, 3H), 2.37 (m, 1H), 2.23 (m, 1H), 1.89 (m, 2H). ^{13}C NMR (100 MHz, D_2O) δ 166.0, 132.1 (2C), 131.6 (2C), 129.2, 127.4, 65.4, 64.9, 57.9, 40.6, 28.1, 23.1. IR (KBr, cm^{-1}) 2980, 1729, 1281, 1115, 686. Anal. Calcd for $C_{13}H_{17}BrClNO_2$: C, 46.66; H, 5.12; N, 4.19. Found: C, 46.60; H, 5.05; N, 4.15.

5.1.8. ((*S*)-1-Methylpyrrolidin-2-yl)methyl 4-chlorobenzoate (5)

Prepared in the similar way as described above in general procedures. (*S*)-1-Methylpyrrolidin-2-yl)methanol (8.0 mmol, 1.0 mL) was added to a solution of 4-chlorobenzoyl chloride (8.0 mmol, 1.1 mL). Yield 1.75 g (82%), mp 227.5–228.3 °C, ^{1}H NMR (400 MHz, D_2O) δ 7.81 (d, *J* = 8.6 Hz, 2H), 7.38 (d, *J* = 8.6 Hz, 2H), 4.61 (dd, *J* = 13.1, *J* = 2.8 Hz, 1H), 4.42 (dd, *J* = 13.0, *J* = 6.5 Hz, 1H),

3.80 (m, 1H), 3.64 (m, 1H), 3.15 (m, 1H), 2.93 (s, 3H), 2.30 (m, 1H), 2.11 (m, 1H), 1.95 (m, 2H). ^{13}C NMR (100 MHz, D_2O) δ 166.0, 138.6, 131.3 (2C), 128.8 (2C), 128.3, 65.4, 64.9, 57.9, 40.6, 28.1, 23.1. IR (KBr, cm^{-1}) 2995, 1737, 1277, 1108, 740. Anal. Calcd for $C_{13}H_{17}Cl_2NO_2$: C, 53.81; H, 5.90; N, 4.83. Found: C, 53,77; H, 5.93; N, 4.79.

5.1.9. ((*S*)-1-Methylpyrrolidin-2-yl)methyl 6-chloronicotinoate (6)

Prepared in the similar way as described above in general procedures. (*S*)-1-methylpyrrolidin-2-yl) methanol (3.0 mmol, 0.35 mL) was added in to a solution of 6-chloronicotinoyl chloride (2.8 mmol, 500 mg). Yield 473 mg (65%), mp 169.3–171.5 °C, ^{1}H NMR (400 MHz, D_2O) δ 8.83 (d, J = 2.3 Hz, 1H), 8.27 (dd, J = 8.3, J = 2.4 Hz, 1H), 7.53 (d, J = 8.4 Hz, 1H), 4.69 (dd, J = 13.1, J = 3.0 Hz, 1H), 4.49 (dd, J = 13.1, J = 6.2) Hz, 1H), 3.82 (m, 1H), 3.65 (m, 2H), 3.15 (m, 1H), 2.93 (s, 3H), 2.31 (m, 1H), 2.11 (m, 1H), 1.96 (m, 2H). ^{13}C NMR (100 MHz, D_2O) δ 166.4, 151.2, 150.7, 139.1, 124.5, 122.6, 66.8, 65.1, 58.5, 41.7, 28.3, 23.2.IR (KBr, cm^{-1}) 2975, 1737, 1677, 1270, 1118, 730. Anal. Calcd for $C_{12}H_{16}Cl_2N_2O_2$: C, 49.50; H, 5.54; N, 9.62. Found: C, 49.58; H, 5.59; N, 9.67.

5.1.10. ((*S*)-1-Methylpyrrolidin-2-yl)methyl 2-quinolinecarboxylate (7)

Prepared in the similar way as described above in general procedures. (*S*)-(−)-1-Methyl-2-pyrrolidinylmethanol (4.0 mmol, 0.5 mL) was added to a solution of 2-quinolinecarboxyl chloride (4.0 mmol, 806 mg). Yield 790 mg (70%), mp 171–174 °C, ^{1}H NMR (400 MHz, D_2O) δ 9.40 (s, 1H), 9.21 (s, 1H), 8.25 (d, J = 8.2 Hz, 1H), 8.13 (d, J = 8.4 Hz, 1H), 7.96 (t, J = 8.2 Hz, J = 7.7 Hz, 1H), 7.75 (t, J = 7.9 Hz, J = 7.5 Hz, 1H), 4.05 (dd, J = 9.0, J = 5.4 Hz, 1H), 3.98 (dd, J = 9.2, J = 5.3 Hz, 1H), 3.19 (m, 1H), 2.52 (s, 3H), 2.32 (m, 1H), 2.06 (m, 1H), 2.09 (m, 1H), 1.82 (m, 3H). ^{13}C NMR (100 MHz, D_2O) δ 167.9, 148.8, 147.5, 138.8, 132.3, 129.7, 128.9, 127.8, 127.5, 122.6, 65.7, 63.9, 55.6, 41.3, 29.1, 22.1. IR (KBr, cm^{-1}) 2995, 1745, 1683, 1278, 1128, 745. Anal. Calcd for $C_{16}H_{19}ClN_2O_2$: C, 62.64; H, 6.24; N, 9.13. Found: C, 62.83; H, 6.61; N, 9.22.

5.1.11. ((*S*)-1-Methylpyrrolidin-2-yl)methyl 4-benzyloxybenzoate (8)

Prepared in the similar way as described above in general procedures. (*S*)-(−)-1-metil-2-pirrolidinilmetanol (3.0 mmol, 0.17 mL) was added into a solution of 4-benzyloxybenzoyl chloride (3.0 mmol, 680 mg). Yield 628 mg (70%), mp 144.3–145.2 °C, ^{1}H NMR (400 MHz, D_2O) δ 7.51 (m, 2H), 7.42 (m, 3H), 7.08 (d, J = 7.5 Hz, 2H), 6.8 (d, J = 7.2 Hz, 2H), 5.16 (s, 2H), 4.62 (d, J = 2.8 Hz, 1H), 4.08 (d, J = 6.6 Hz, 1H), 3.78 (t, J = 4.2 Hz, 1H), 3.62 (t, 2H), 3.13 (m, 2H), 2.92 (s, 3H), 2.14 (m, 1H), 2.02 (m, 1H). ^{13}C NMR (100 MHz, D_2O) δ 166.0, 165.0, 141.2, 130.9 (2C), 129.0 (2C), 127.7, 127.2 (2C), 122.5, 114.2 (2C), 70.9, 65.4, 64.9, 57.9, 40.6, 28.1, 23.1. IR (KBr, cm^{-1}) 2988, 1730, 1269, 1220, 1119. Anal. Calcd for $C_{20}H_{24}ClNO_3$: C, 66.38; H, 6.69; N, 3.87. Found: C, 66.56; H, 6.81; N, 3.95.

5.1.12. ((*S*)-1-Methylpyrrolidin-2-yl)methyl 6-benzyloxynicotinoate (9)

Prepared in the similar way as described above in general procedures. (*S*)-(−)-1-metil-2-pirrolidinilmetanol (3.0 mmol, 0.17 mL) was added into a solution of 4-benzyloxynicotinoyl chloride (3.0 mmol, 680 mg.). Yield 628 mg (70%), mp 144.3–145.2 °C, ^{1}H NMR (400 MHz, D_2O) δ 7.51 (m, 2H), 7.42 (m, 3H), 7.08 (d, J = 7.5 Hz, 2H), 6.8 (d, J = 7.2 Hz, 2H), 5.16 (s, 2H), 4.62 (d, J = 2.8 Hz, 1H), 4.08 (d, J = 6.6 Hz, 1H), 3.78 (t, J = 4.2 Hz, 1H), 3.62 (t, 2H), 3.13 (m, 2H), 2.92 (s, 3H), 2.14 (m, 1H), 2.02 (m, 1H). ^{13}C NMR (100 MHz, D_2O) δ 166.0, 165.0, 141.2, 130.9 (2C), 129.0 (2C), 127.7, 127.2 (2C), 122.5, 114.2 (2C), 70.9, 65.4, 64.9, 57.9, 40.6, 28.1, 23.1. IR (KBr, cm^{-1}) 2995, 1747, 1672, 1278, 1248, 1115. Anal. Calcd for $C_{20}H_{24}ClNO_3$: C, 66.38; H, 6.69; N, 3.87. Found: C, 66.56; H, 6.81; N, 3.95.

Acknowledgments

This work was partially funded by FONDECYT Grants 1100542 and 11100177 and ICM Grant MSI 10-063-F NEDA, and supported by Project ICM-P10-003-F CILIS, granted by Fondo de Innovación para la Competitividad del Ministerio de Economía, Fomento y Turismo, Chile.

References and notes

1. Le Novère, N.; Changeux, J. P. *Nucleic Acids Res.* **1999**, *27*, 340.
2. Zoli, M.; Le Novère, N.; Hill, J.; Changeux, J. P. *J. Neurosci.* **1995**, *15*, 1912.
3. Le Novère, N.; Corringer, P. J.; Changeux, J. P. *J. Neurobiol.* **2002**, *53*, 447.
4. Albuquerque, E. X.; Pereira, E. F. R.; Alkondon, M.; Rogers, S. W. *Physiol. Rev.* **2009**, *89*, 73.
5. Chavez-Noriega, L. E.; Crona, J. H.; Washburn, M. S.; Urrutia, A.; Elliott, K. J.; Johnson, E. C. *J. Pharmacol. Exp. Ther.* **1997**, *280*, 346.
6. Paterson, D.; Nordberg, A. *Prog. Neurobiol.* **2000**, *61*, 75.
7. Sher, E.; Chen, Y.; Sharples, T. J.; Broad, L. M.; Benedetti, G.; Zwart, R.; McPhie, G. I.; Pearson, K. H.; Baldwinson, T. *Curr. Top. Med. Chem.* **2004**, *4*, 283.
8. Wonnacott, S. *Trends Neurosci.* **1997**, *20*, 92.
9. Wonnacott, S. *Trends Pharmacol. Sci.* **1990**, *11*, 216.
10. Jensen, A.; Frølund, B.; Liljefors, T.; Krogsgaard-Larsen, P. *J. Med. Chem.* **2005**, *48*, 4705.
11. Gotti, C.; Moretti, M.; Gaimarri, A.; Zanardi, A.; Clementi, F.; Zoli, M. *Biochem. Pharmacol.* **2007**, *74*, 1102.
12. Picciotto, M. R.; Zoli, M.; Rimondini, R.; Lena, C.; Marubio, L.; Pich, E.; Fuxe, K.; Changeaux, J. P. *Nature* **1998**, *391*, 173.
13. Newhouse, P.; Singh, A.; Potter, A. *Curr. Top. Med. Chem.* **2004**, *4*, 267.
14. Shytle, R. D.; Silver, A.; Lukas, R. J.; Newman, M. B.; Sheehan, D. V.; Sanberg, P. R. *Mol. Psychiatry* **2002**, *7*, 525.
15. Romanelli, M. N.; Gualtieri, F. *Med. Res. Rev.* **2003**, *23*, 393.
16. Wonnacott, S.; Barik, J. *Tocris Sci. Rev. Ser.* **2007**, *6*, 1.
17. Daly, J. W. *Cell. Mol. Neurobiol.* **2005**, *25*, 513.
18. Brejc, K.; Van Dijk, W. J.; Klaassen, R. V.; Schuurmans, M.; Van Der Oost, J.; Smit, A. B.; Sixma, T. K. *Nature* **2001**, *411*, 269.
19. Celie, P. H. N.; Van Rossum-Fikkert, S. E.; Van Dijk, W. J.; Brejc, K.; Smit, A. B.; Sixma, T. K. *Neuron* **2004**, *41*, 907.
20. Rucktooa, P.; Smit, A. B.; Sixma, T. K. *Biochem. Pharmacol.* **2009**, *78*, 777.
21. Hansen, S. B.; Sulzenbacher, G.; Huxford, T.; Marchot, P.; Taylor, P.; Bourne, Y. *Eur. Mol. Biol. Organ. J.* **2005**, *24*, 3635.
22. Unwin, N. *J. Mol. Biol.* **2005**, *346*, 967.
23. Sine, S. M.; Engel, A. G. *Nature* **2006**, *440*, 448.
24. Grady, S. R.; Drenan, R. M.; Breining, S. R.; Yohannes, D.; Wageman, C. R.; Fedorov, N. B.; McKinney, S.; Whiteaker, P.; Bencherif, M.; Lester, H. A.; Marks, M. J. *Neuropharmacology* **2010**, *58*, 1054.
25. Xiu, X.; Puskar, N. L.; Shanata, J. A.; Lester, H. A.; Dougherty, D. A. *Nature* **2009**, *458*, 534.
26. Scriabine, A. *CNS Drugs Rev.* **1999**, *5*, 395.
27. Fischer, E.; Speier, A. *Chemische Derichte* **1895**, *28*, 3252.
28. Batcho, A.; Leimgruber, W. *Org. Synth.* **1990**, *7*, 34.
29. Anderson, D.; Arneric, S. *Eur. J. Pharmacol.* **1994**, *253*, 261.
30. Peng, X.; Katz, M.; Gerzanich, V.; Anand, R.; Lindstrom, J. *Mol. Pharmacol.* **1994**, *45*, 546.
31. Peng, J.; Fryer, J. D.; Hurst, R. S.; Schroeder, K. M.; George, A. A.; Morrissy, S.; Groppi, V. E.; Leonard, S. S.; Lukas, R. J. *J. Pharmacol. Exp. Ther.* **2005**, *313*, 24.
32. Pacheco, M.; Pastoor, T.; Lukas, R.; Wecker, L. *Neurochem. Res.* **2001**, *26*, 683.
33. Houlihan, L. M.; Slater, Y.; Guerra, D. L.; Peng, J. H.; Kuo, Y. P.; Lukas, R. J.; Cassels, B. K.; Bermudez, I. *J. Neurochem.* **2001**, *78*, 1029.
34. Moroni, M.; Zwart, R.; Sher, E.; Cassels, B. K.; Bermudez, I. *Mol. Pharmacol.* **2006**, *70*, 755.
35. Carbone, A. L.; Moroni, M.; Groot-Kormelink, P. J.; Bermudez, I. *Br. J. Pharmacol.* **2009**, *156*, 970.
36. Kuryatov, A.; Berrettini, W.; Lindstrom, J. *Mol. Pharmacol.* **2011**, *79*, 119.
37. Gotti, C.; Moretti, M.; Meinerz, N. M.; Clementi, F.; Gaimarri, A.; Collins, A. C.; Marks, M. J. *Mol. Pharmacol.* **2008**, *73*, 1796.
38. Akk, G. *J. Physiol.* **2001**, *535*, 729.
39. Mazzaferro, S.; Benallegue, N.; Carbone, A.; Gasparri, F.; Vijayan, R.; Biggin, P. C.; Moroni, M.; Bermudez, I. *J. Biol. Chem.* **2011**, *286*, 31043.
40. Thompson, J.; Higgins, D.; Gibson, T. *Nucleic Acids Res.* **1994**, *22*, 4673.
41. Sali, A.; Blundell, T. L. *J. Mol. Biol.* **1993**, *234*, 779.
42. Shaw, D. Desmond Molecular Dynamics System, v 3.0, New York, NY, 2011.
43. Maestro Desmond Interoprability Tools, v. 3.0, New York, NY, 2011.
44. Berendsen, H.; Postma, J.; Gunsteren, W.; Hermans, J. *Intermolecular Forces* **1981**, *331*, 331.
45. Muñoz, C.; Adasme, F.; Alzate-Morales, J. H.; Vergara-Jaque, A.; Kniess, T.; Caballero, J. *J. Mol. Graph. Model.* **2012**, *32*, 39.
46. Morris, G. M.; Goodsell, D. S.; Halliday, R. S.; Huey, R.; Hart, W. E.; Belew, R. K.; Olson, A. J. *J. Comput. Chem.* **1998**, *19*, 1639.